Measurements of the electron impact ionisation cross sections of He, C, O and N atoms

1978 J. Phys. B: At. Mol. Phys. 11 3115

(http://iopscience.iop.org/0022-3700/11/17/021)

J. Phys. B: Atom. Molec. Phys., Vol. 11, No. 17, 1978. Printed in Great Britain

Measurements of the electron impact ionisation cross sections of He, C, O and N atoms

E Brook†‡, M F A Harrison† and A C H Smith†‡

† Euratom/UKAEA Fusion Association, Culham Laboratory, Abingdon, Oxfordshire OX14 3DB, England

Received 28 March 1978

Abstract. Absolute measurements are reported of the electron impact ionisation cross sections of ground-state atoms of helium, carbon, nitrogen and oxygen for electron energies ranging from 7 to 1000 eV. The method used was that of crossed beams in which fast beams of atoms are produced by charge capture of 2 to 4 keV ions in a gas target. The data for helium atoms above 100 eV are in excellent agreement (±5%) with the absolute data of Rapp and Englander-Golden who used a static gas target technique. However, the present data are smaller in magnitude at lower energies. Data for oxygen and nitrogen atoms are in adequate agreement with data from earlier crossed-beams experiments that employed thermal-energy atom beams. Comparisons are made with the various published theoretical cross sections.

1. Introduction

Data on electron impact ionisation of atmospheric atoms are obviously of interest for atmospheric physics and for related applications such as telecommunications and space-vehicle re-entry. They are also important in plasma chemistry and they are of direct relevance to the contamination of nuclear fusion devices by impurity elements such as C and O (Harrison 1977).

Previous measurements of the electron impact ionisation cross sections of O (Fite and Brackmann 1959, Boksenberg 1961, Rothe *et al* 1962) and also of N (Smith *et al* 1962) have been based upon a crossed-beams approach. In these experiments mono-energetic electrons are passed through a beam of thermal-energy atoms and molecules, the latter emanating from a source in which molecular gas is partially dissociated by either a pulsed or radiofrequency discharge. Such measurements are essentially relative in nature, each apparatus being calibrated by measuring the ionisation arising from a beam of undissociated molecules and applying the molecular ionisation data of Tate and Smith (1932) to the results. Data for atoms are then obtained by initiating the discharge and measuring the ionisation and degree of dissociation of the beam leaving the source.

Peterson (1964) sought to make absolute crossed-beams measurements for N atoms by using a fast atom beam produced by charge exchange of 2 keV N^+ in

‡ Department of Physics and Astronomy, University College London, Gower Street, London WC1E 6BT, England.

0022-3700/78/0017-3115 $03.00

a N_2 gas target. In principle the flux of such energetic atoms can be measured absolutely and hence absolute values of the cross section can be determined. Unfortunately Peterson's pioneering data suffered from apparatus effects which are now better understood and can be avoided. The present work is based on a similar approach and this paper describes measurements of the cross sections for O and N made using crossed beams of electrons and fast atoms. The technique offers a further advantage insofar as ions of any element can be neutralised to form fast atom beams. This aspect is exemplified by the present measurements on C atoms. The only other experimental data for C (Wang and Crawford 1971) are not published but have been reported by Barnett *et al* (1976); it is presumed that their technique for C atoms is similar to that used for Ag atoms (Crawford and Wang 1967), namely a crossed electron and thermal atom beam approach.

The electron impact ionisation cross sections of O, N and C atoms have been calculated using several variants of the Born approximation by Peach (1970, 1971), Omidvar *et al* (1972), McGuire (1971) and for O atoms by Kazaks *et al* (1972). A Bethe approximation, scaled empirically, has been applied to O and N atoms by Seaton (1959).

The earlier thermal-beam data for O and N rely upon a knowledge of the ionisation cross sections for O_2 and N_2 molecules that have been measured by passing a magnetically collimated electron beam through a static gas target. Some sources of error in this method can arise due to uncertainties in the density and length of the gas target. The latter arise from any electrons that have helical trajectories within the collimating magnetic field (Kieffer and Dunn 1966) and this effect appears to be more significant at the lower electron energies. The magnetically collimated electron beam and static gas target technique has been refined by Rapp and Englander-Golden (1965) and their absolute cross section data are customarily accepted as definitive for rare-gas atoms and many common molecules. In the present fast atom beam technique the electron beam is carefully shielded from magnetic fields and the target thickness is precisely defined. Thus it is valuable to compare the Rapp and Englander-Golden data with corresponding data obtained by the electron and fast atom beams technique. For either technique a measurement of the cross section for the ionisation of ground state He atoms presents a minimum of uncertainties and so such a measurement is included in the present set of fast atom beam studies.

2. Apparatus and method

Both the apparatus and the method used for fast atom beam studies of metastable atoms have been described by Dixon *et al* (1975, 1976). The same apparatus, shown in simple schematic form in figure 1, has been used for the present studies in which fast atoms are formed predominantly in their ground states by charge exchange of singly charged parent ions in a gas cell. This cell is 70 mm long and it is filled to a density of about 4×10^{18} m^{-3}. The target gas is selected on the basis of minimum energy defect, $\Delta\chi$, for charge exchange into the ground state of each fast atomic species; also monatomic gases are preferred with a view to minimising the number of charge-exchange channels that can result in fast excited atoms. The combinations used are shown in table 1.

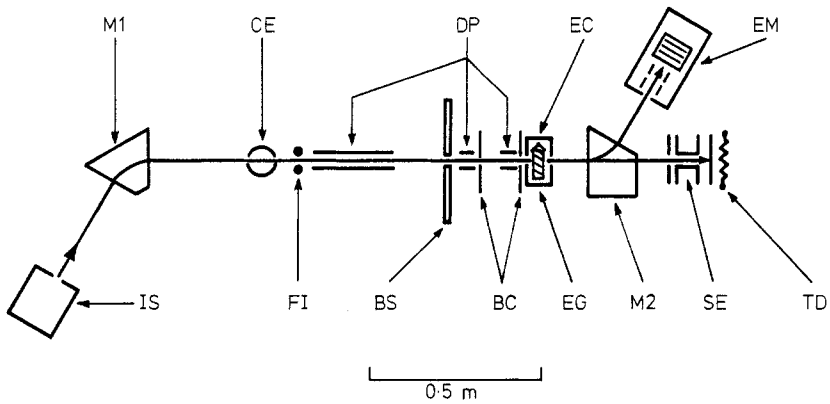

Figure 1. Simplified diagram of the fast atom-beam and crossed electron-beam apparatus. IS, ion source; M1, selector magnet; CE, charge-exchange gas cell; FI, field-ioniser wires; DP, deflector plates; BS, beam stop; BC, beam collimators; EG, electron gun; EC, electron collector; M2, analyser magnet; SE, secondary electron detector; TD, thermopile detector; EM, electron multiplier.

Fast atoms leaving the gas cell travel about 0·75 m before crossing the electron beam and so the time taken by O, N and C in the energy range 2–4 keV is about 3 to 5 μs. Thus any short-lived excited states have ample time to decay radiatively. Any long-lived highly excited atoms ($n \gtrsim 13$) are ionised in an electrostatic field and deflected out of the beam, so that only metastable atoms and those in long-lived states with $8 \lesssim n \lesssim 12$ can affect the measurements. High magnetic fields are needed to mass select the parent ions and to separate the product ions of the relatively massive atmospheric elements and these necessitate improved magnetic shielding of the electron gun to maintain fields of less than $0{\cdot}5 \times 10^{-4}$ T in the collision region. Limitations in the available intensity of these magnetic fields and the convenience of long transit times dictate that the energies of the fast atom beams should lie in the region 1 to 4 keV. A further advantage of using these relatively low-energy beams is that the probability for ionisation of the atmospheric atoms in collisions with residual gas is then small. In the present experiment the background from this spurious ionisation was usually less than three times the signal from true electron impact ionisation.

The ions are detected as single particles by a calibrated electron multiplier (Dance *et al* 1967) and the true signal is separated from the spurious background by conventional pulsed modulation of the crossed beams (Harrison 1968). The output pulses from the multiplier are fed to a pair of scalers so gated in synchronism with the beam modulation that one scaler accumulates, over an experimental period t (usually 100 s), the pulses due to the true ionisation plus spurious backgrounds and the other

Table 1.

Parent ion	Target gas	$\Delta\chi$ (eV)
O^+	Kr	+0·38
N^+	Ar	+1·21
C^+	Xe	+0·87
He^+	He	0

scaler accumulates pulses due to the backgrounds alone. The difference in scaler readings, corrected for the dead time of the single-particle counting system, is thus the total number, S, of product ions produced in the experimental period t.

The electron-beam current J is measured absolutely and so is the equivalent current I_0 of the atom beam. This latter parameter is determined by the power that the atom beam deposits upon a sensitive vacuum thermopile whose sensitivity ϵ is regularly measured by directing onto it ion beams of known current and energy (Dixon *et al* 1976). This thermopile is subject to slight thermal drifts during the experimental period (t) and so the parameter actually observed during a cross section measurement is I_{e0}, the current of secondary electrons produced by impact of the fast atom beam upon a thin film of aluminium that is in good thermal contact with the thermopile and yet electrically isolated from it. The equivalent current is determined from $I_0 = I_{e0}/\gamma_0$, where γ_0 is the secondary emission coefficient. The thermopile is sufficiently stable to allow accurate measurements of γ_0 so that frequent measurements of these coefficients were made throughout the present studies.

Both J and I_{e0} are measured using DC instruments and so, if the beams are pulse modulated, the actual values recorded are $\bar{J} = \alpha_J J$ and $\bar{I}_{e0} = \alpha_0 I_{e0}$ where the overbars denote averaging over the duty cycles α_J and α_0 of the electron and atom beams. These beam currents might drift very slightly during the experimental periods and this effect is overcome by feeding the signals from the beam currents into amplitude to pulse-rate convertors and using scalers to count these pulses for each period. Thus values of $\bar{J}$ and $\bar{I}_{e0}$ integrated over each period (t) can be derived.

In a modulated crossed-beams experiment the measured ionisation cross section for atoms, $Q_m(E)$ at incident electron energy E, can be determined from

$$Q_m(E) = \frac{S}{t\Omega\alpha_s}\frac{\gamma_0\alpha_0}{\bar{I}_{e0}}\frac{\alpha_J\beta}{\bar{J}}\frac{vV}{(v^2+V^2)^{1/2}}e^2h'. \tag{1}$$

Here α_s is the duty cycle for the gating period of the scalers used to record the ionisation events and Ω is the efficiency of the electron multiplier; v and V are, respectively, the velocities of the electrons and the atoms and e is the electronic charge. The parameter h' is the effective height of the beam collision region and is measured by sampling the current profiles of the beams. The factor β depends upon the particular sequence of pulsed modulation of the beams. If the backgrounds arise solely from processes associated with the fast atom beam then only the electron beam need be pulsed (Harrison 1968) and $\beta = \alpha_s/\alpha_J$. Most of the present data were obtained in this manner, the electron beam being pulsed on for 250 μs with a 50% duty cycle. The scalers were gated to count for 240 μs within the appropriate pulses of the electron beam. Checks were made at higher modulation frequencies, the respective beam pulse and gate lengths then being 25 μs and 15 μs, but no significant changes were observed in the data. If the electron beam also introduces spurious background counts then modulation of both beams is required and the factor $\beta = 1$. Checks were made using modulation of both beams (see table 2) but no significant effects were observed.

The equivalent atom-beam currents were about 10^{-9} A and $\bar{J}$ ranged from 10 μA to 2 mA. The total count rate (true signal plus background) was only a few hundred counts per second and so no dead time corrections were required. The secondary emission coefficient ($\gamma_0 \simeq 1{\cdot}2$ to $2{\cdot}0$) and the sensitivity of the thermopile ($\epsilon \simeq 6\ \mu V\ \mu W^{-1}$) became stable for each particular atom beam after a few days of operation and then both varied by less than 4% over each set of cross section data.

As a further consistency check, data were taken with both 2 keV and 4 keV atom beams but no changes were observed. The efficiency Ω of the electron multiplier was in the range 0·84 to 0·97 depending upon the atom species and energy but it varied by less than $\pm 0{\cdot}02$ throughout each set of data. The value of the contact potential within the electron gun was assessed from both the present and previous data for ionisation thresholds measured in this apparatus and a value of 3·2 V is accepted throughout this paper; however, the contact potential is uncertain within the limits 2·2 to 3·5 V.

The electron-beam energy ranged from about 10 eV to 1 keV and at most electron energies the magnitudes of S were measured for at least 5 values of $\bar{J}$. The cross section and its 90% confidence limits were then determined using a least-squares fit for the relationship

$$Q_m(E)C\bar{J} = \frac{Sh'\gamma_0}{t\Omega I_{e0}} \tag{2}$$

where the constant C contains known parameters from equation (1). Exceptions to this procedure occur at electron energies below about 50 eV where single values of $\bar{J}$ were generally used and any drifts in the sensitivities of the detectors corrected by normalisation to absolute measurements of the cross sections at a convenient higher energy (see tables 2 and 4 to 6).

Low-energy secondary electrons can be produced within the electron gun but these can be excluded from the beam collision region by suitable repelling potentials (see figure 2 of Dixon *et al* 1976). The diagnostic technique of biasing the collision region was repeatedly invoked during the present measurements but the cross section data were unaffected.

One problem previously encountered in studies employing singly charged ions produced by electron impact on molecular gases is the presence of doubly charged molecular ions such as N_2^{2+} which are not separated from the parent (e.g. N^+) beam (see Harrison *et al* 1963). In the present experiment such molecular ions might contaminate the atom beam with small numbers of neutral molecules (e.g. N_2). The presence of contaminating molecules can be detected by observing any singly charged molecular ions (e.g. N_2^+) that arise from collisions with the crossed electron beam. Although very small signals were observed their contribution to the measured cross sections was less than 1% and so molecular-ion effects were neglected.

The systematic errors in the magnitude of the cross sections were assessed on the basis of uncertainties in calibrations and any variation in performance that occurred between calibrations. The estimated errors were $S(\pm 3\%)$, $\gamma_0(\pm 1\%)$, $\bar{I}_{e0}(\pm 1\%)$ and $h'(\pm 0{\cdot}5\%)$. Uncertainties in $\bar{J}$ were dependent upon the energy of the electron beam, ranging from about $\pm 15\%$ at 10 eV to 5% at 25 eV, above these energies the uncertainties became very small, being only 0·25% at 1 keV. Errors in the other parameters of equation (1) were negligible.

3. Results and discussion

3.1. Ionisation of helium atoms

Measurements were made over a range of incident electron energies from 11 to 997 eV and both 2 and 4 keV atom beams were used. The data are presented in figure 2

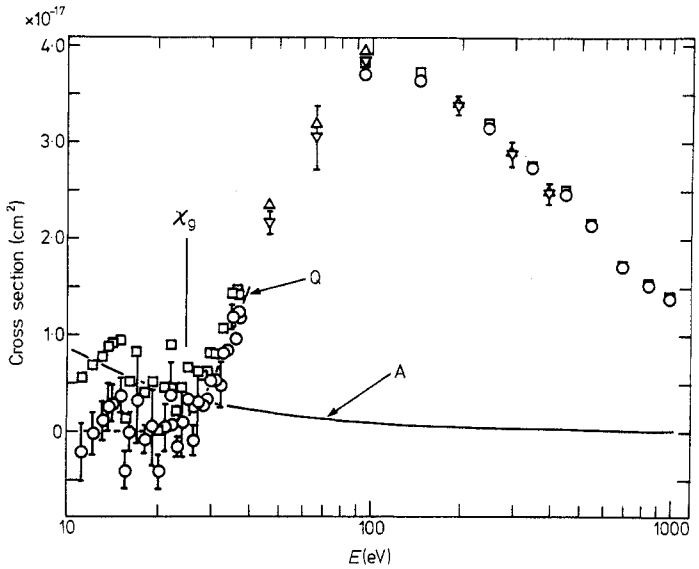

Figure 2. Ionisation of helium atoms. The measured cross section $Q_m(E)$ is shown by △ for 2 keV beams and □ for 4 keV beams. The corresponding symbols for the true ionisation cross section $Q(E)$ are ▽ and ○. The error bars are shown only for $Q(E)$ and are defined in table 2. The apparent cross section for ionisation of long-lived excited He atoms in the beam, $Q_u^*(E)$ = constant × E^{-1}, is determined by fitting to $Q_m(E)$ at energies below the ground-state threshold χ_g. The values $\bar{Q}_u^*(E)$ extrapolated to higher energies are shown by curve A. For convenience a smooth curve (Q) is drawn through the low-energy data for $Q(E)$.

Table 2. Electron impact ionisation of helium.

Mean electron energy† (eV)	$Q_m(E)$ (10^{-17} cm^2)	$Q(E)$‡ (10^{-17} cm^2)	Random errors§ (10^{-17} cm^2)
11·3	0·55	−0·22	(0·31)
12·3	0·69	−0·02	(0·22)
13·3	0·77	0·11	(0·20)
13·8	0·88	0·25	(0·25)
14·3	0·90	0·29	(0·19)
15·3	0·94	0·37	(0·19)
15·8	0·14	−0·41	(0·20)
16·3	0·52	−0·01	(0·21)
17·3	0·82	0·32	(0·45)
18·3	0·40	−0·08	(0·15)
19·3	0·51	0·06	(0·42)
20·3	0·01	−0·42	(0·19)
21·3	0·45	0·04	(0·25)
22·3	0·77	0·38	(0·34)
22·3	0·44	0·05	(0·11)
23·3	0·21	−0·16	(0·11)

Table 2. (continued)

Mean electron energy† (eV)	$Q_m(E)$ (10^{-17} cm^2)	$Q(E)$‡ (10^{-17} cm^2)	Random errors§ (10^{-17} cm^2)
(a)			
24·3	0·45	0·09	(0·36)
25·3	0·67	0·33	(0·11)
26·3	0·23	−0·10	(0·16)
27·3	0·62	0·30	(0·40)
28·3	0·58	0·27	(0·08)
29·3	0·63	0·33	(0·11)
30·3	0·81	0·52	(0·06)
31·3	0·81	0·53	(0·08)
32·3	0·76	0·49	(0·24)
33·3	1·07	0·81	(0·07)
34·3	1·09	0·84	(0·07)
35·3	1·43	1·18	(0·13)
36·3	1·20	0·96	(0·06)
37·3	1·47	1·24	(0·07)
(b)			
37·3	1·42	1·18	0·06
47*	2·34	2·16	0·12
67*	3·18	3·05	0·33
97*	3·93	3·84	0·08
97	3·79	3·70	0·09
147	3·71	3·65	0·09
197*	3·42	3·38	0·10
247	3·20	3·16	0·05
297*	2·91	2·88	0·13
347	2·77	2·75	0·04
397*	2·49	2·47	0·11
447	2·49	2·47	0·08
547	2·16	2·15	0·02
697	1·72	1·71	0·03
847	1·53	1·52	0·03
997	1·38	1·37	0·03

† Mean electron energy ± 1·0 eV.
(a) The apparent cross section $Q_a^* \simeq$ constant × E^{-1} was determined by least-squares fitting to data at energies below (a).
(b) All measurements below (b) were made absolute by normalisation to the absolute value of $Q_m(E)$ measured at 97 eV using a 4 keV atom beam.
* Data obtained using a 2 keV atom beam and with both beams pulsed. All other data were obtained using a 4 keV atom beam and with only the electron beam pulsed.
‡ The true ionisation cross section determined from $Q(E) = Q_m(E) - \overline{Q}_a^*(E)$.
§ 90% confidence limits except for bracketed values that are standard errors of the mean.

and table 2. It should be noted that the measurements yield an apparent ionisation cross section at electron energies below the ground-state threshold energy (χ_g). This anomaly is attributed to a small population of long-lived excited atoms in the beam. Presumably, such atoms are formed, together with ground-state atoms, by charge capture in the gas cell. In the case of helium beams the atoms might be in metastable states but comparable measurements were made using a 4 keV beam of H atoms

and in this case any metastable H(2S) would have been quenched by the electric fields along the flight path to the collision region. This experiment yielded an even larger apparent cross section below the hydrogen ground-state threshold. Further, it can be seen in §3.2 that the corresponding apparent cross sections for O, N and C beams are very small. It therefore seems reasonable to assume that the ionisation of helium below the ground-state threshold arises not from metastable atoms in the beam but rather from a small population of atoms excited to long-lived states with (see §2) $8 \lesssim n \lesssim 12$. The magnitudes of these apparent cross sections should therefore be dependent upon the excited-atom populations and the ratio of the state lifetimes to atom transit times. The ionisation thresholds (χ_n) of such states are much smaller than χ_g (i.e. $\chi_n \simeq \chi_g/n^2$), so that the apparent cross section $Q_a^*(E)$, measured over the experimental range of E below χ_g, demonstrates the high-energy dependence of ionisation from those atoms in high-n states. Unfortunately the present data are too scattered to permit a positive identification of the energy dependence for the He beam but the classical E^{-1} form is favoured and it is assumed in this paper. Using this assumption it is possible to extrapolate the apparent ionisation cross section to incident energies greater than χ_g and hence correct the measured cross section using the expression $Q(E) = Q_m(E) - \bar{Q}_a^*(E)$ where $Q(E)$ is the true cross section for ionisation from the ground-state. Here $E > \chi_g$ and $\bar{Q}_a^*(E)$ represents the extrapolated values of the apparent cross section for ionisation. $Q_a^*(E)$ is measured below χ_g and is fitted by the least-squares method to a curve (see A of figure 2) of the form $Q_a^*(E) = \text{constant} \times E^{-1}$. The magnitudes of both $Q_m(E)$ and $Q(E)$ are listed in table 2. The correction to $Q_m(E)$ is substantial near to the ground-state threshold but decreases rapidly with increasing electron energy; for example it is only 3·5% of $Q_m(E)$ at the peak of the cross section.

In figure 3 the true cross section, $Q(E)$, is compared with corresponding data measured using the technique of a static gas target and a magnetically collimated electron beam. The data of Rapp and Englander-Golden (1965) are generally regarded as being the most accurate available for He atoms (Kieffer and Dunn 1966) and are used here for the comparison. Such experiments rely on the collection of all

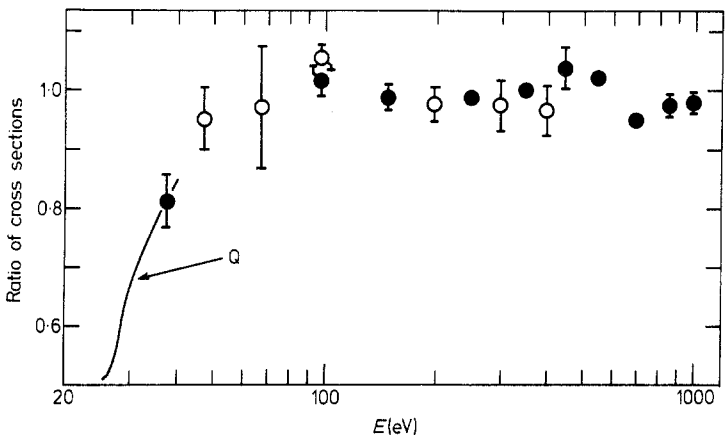

Figure 3. The ratio of $Q(E)$ for helium atoms to the gas target data of Rapp and Englander-Golden. Data for the 2 keV atom beams are shown by ○ and for the 4 keV beam by ●. The error bars represent only uncertainties in the present fast atom beam data. For convenience the ratios at low energies are shown by curve (Q) that corresponds to the cross section curve (Q) of figure 2.

ions formed in the gas cell and so the measured cross section includes small contributions from He^{2+}. The data of Stanton and Monahan (1960) have been used to allow for these contributions. At energies greater than 100 eV there is remarkable agreement (better than $\pm 5\%$) between the fast atom beam and static gas target data, thereby demonstrating the excellent precision of the calibration techniques used for measuring target thicknesses and beam currents in each of these widely differing methods. However, at lower electron energies the fast atom beam data become progressively smaller than those of the static target experiment and approach a ratio of 0·5 close to the ground-state threshold. This discrepancy cannot be explained by the allowances made for the population of excited atoms in the fast He atom beam data and it is therefore concluded that the static gas target data overestimate the ionisation cross section at low electron energies.

Magnetic collimation of the electron beam is needed in a static gas target experiment to exclude electrons from the ion collector. It has frequently been emphasised (for example, Kieffer and Dunn 1966) that this method is susceptible to errors from any electrons that follow helical trajectories through the gas target cell. The cross sections measured in various static target experiments, especially in targets of Ne and Ar, differ appreciably at low energies and this may be due to helical trajectories. Amongst these data the measurements of Rapp and Englander-Golden are invariably the smallest but the present comparison of their He data with those from a fast atom beam crossing a magnetically shielded electron beam indicate that the inherent problems of magnetic collimation were not fully overcome. On the one hand this uncertainty raises doubts as to the accuracy of data for other atoms and molecules measured using the static gas target technique and on the other it emphasises the importance of eliminating ambiguities in low-energy data obtained using the present technique.

3.2. Low-energy data for O, N and C atoms

In each of these measurements there is evidence of a very small apparent cross section below the ground-state threshold, presumably due to ionisation contributions from long-lived excited atoms. However, to interpret the low-energy behaviour of these relatively complex atoms it is first necessary to consider the various channels for inner- and outer-shell ionisation and also autoionisation. The most significant of these, together with their thresholds, are listed for both ground-state and metastable atoms in table 3. The lowest threshold for ionisation of oxygen atoms (from the ^{1}S metastable state) lies at 12·8 eV and so data at energies below 12 eV have been used to determine $Q_a^*(E)$ for the population of long-lived excited atoms in the oxygen atom beam. This apparent cross section is shown by curve B in figure 4(*a*) which also shows $Q(E)$. Both $Q_m(E)$ and $Q(E)$ are listed in table 4 for incident electron energies ranging from 7·9 eV to 997 eV and for both 2 and 4 keV atom beams. The magnitude of $Q_a^*(E)$ is very small, amounting to only 0·3% at the peak of $Q_m(E)$. The present apparatus does not have good resolution of electron-beam energies ($\simeq 70\%$ of the electrons within $\pm 0{\cdot}75$ eV: Dance *et al* 1966) and to this must be added uncertainties in contact potentials (see §2). Thus, although the onset of ionisation appears in the region of the ^{3}P ground-state threshold, it is not practicable to resolve contributions from atoms in the ^{1}S metastable state, or the 14·1 eV threshold for excitation from the ground state to the ^{3}D autoionising state. Any contributions from atoms in the ^{1}D metastable state (at 15·0 eV) are too small to observe

Table 3. Ionisation channels for O, N and C atoms.

Oxygen		
$O(1s^2 2s^2 2p^4)^3P(g)$	[o; 13·61 eV]	$\rightarrow O^+(1s^2 2s^2 2p^3)^4S$
	[i; 28·5 eV]	$\rightarrow O^+(1s^2 2s 2p^4)^4P$
	[e; 14·1 eV]	$\rightarrow O(1s^2 2s 2p^4 3p)^3D - [a] \rightarrow O^+(1s^2 2s^2 2p^3)^4S$
$O(1s^2 2s^2 2p^4)^1D(m)$	[o; 15·0 eV]	$\rightarrow O^+(1s^2 2s^2 2p^3)^2D$
	[i; 32·2 eV]	$\rightarrow O^+(1s^2 2s 2p^4)^2D$
$O(1s^2 2s^2 2p^4)^1S(m)$	[o; 12·8 eV]	$\rightarrow O^+(1s^2 2s^2 2p^3)^2D$
	[i; 29·8 eV]	$\rightarrow O^+(1s^2 2s 2p^4)^2D$
Nitrogen		
$N(1s^2 2s^2 2p^3)^4S(g)$	[o; 14·53 eV]	$\rightarrow N^+(1s^2 2s^2 2p^2)^3P$
	[i; 20·4 eV]	$\rightarrow N^+(1s^2 2s 2p^3)^5S$
	[e; 17·9 eV]	$\rightarrow N(1s^2 2s 2p^3 3p)^4P - [a] \rightarrow N^+(1s^2 2s^2 2p^2)^3P$
$N(1s^2 2s^2 2p^3)^2D(m)$	[o; 12·2 eV]	$\rightarrow N^+(1s^2 2s^2 2p^2)^3P$
	[i; 23·6 eV]	$\rightarrow N^+(1s^2 2s 2p^3)^3D$
$N(1s^2 2s^2 2p^3)^2P(m)$	[o; 11·0 eV]	$\rightarrow N^+(1s^2 2s^2 2p^2)^3P$
	[i; 22·4 eV]	$\rightarrow N^+(1s^2 2s 2p^3)^3D$
Carbon		
$C(1s^2 2s^2 2p^2)^3P(g)$	[o; 11·26 eV]	$\rightarrow C^+(1s^2 2s^2 2p)^2P$
	[i; 16·6 eV]	$\rightarrow C^+(1s^2 2s 2p^2)^4P$
	[e; 12·1 eV]	$\rightarrow C(1s^2 2s 2p^3)^1D$ } $- [a] \rightarrow C^+(1s^2 2s^2 2p)^2P$
	[e; 13·1 eV]	$\rightarrow C(1s^2 2s 2p^3)^3S$ }
$C(1s^2 2s^2 2p^2)^1D(m)$	[o; 10·0 eV]	$\rightarrow C^+(1s^2 2s^2 2p)^2P$
	[i; 19·3 eV]	$\rightarrow C^+(1s^2 2s 2p^2)^2D$
$C(1s^2 2s^2 2p^2)^1S(m)$	[o; 8·6 eV]	$\rightarrow C^+(1s^2 2s^2 2p)^2P$
	[i; 17·9 eV]	$\rightarrow C^+(1s^2 2s^2 2p)^2D$
$C(1s^2 2s 2p^3)^5S(m)$	[o; 12·4 eV]	$\rightarrow C^+(1s^2 2s 2p^2)^4P$

Symbols
g ground state
m metastable state
o outer-shell ionisation
i inner-shell ionisation
e excitation
a autoionisation.

although there is slight evidence of inner-shell ionisation from the ground state at 28·5 eV as can be seen from the smooth curve drawn through the $Q(E)$ data points in figure 4(*a*).

Interpretation of the low-energy data for nitrogen atoms is complicated by the low-lying thresholds for the metastable states (^2P at 11·0 eV and ^2D at 12·2 eV) and it is considered that the amount and precision of the data lying below 11 eV are not adequate to yield a meaningful value of $Q_a^*(E)$. However, it is noted that both N and O atoms have comparable transit times through the apparatus and so the populations of their long-lived excited atoms are also likely to be comparable. It is therefore reasonable to extrapolate the apparent cross section measured for the O beam to the data for the N atom beam and so the following scaling procedure has been adopted,

$$Q_{aN}^*(\epsilon_N) = Q_{aO}^*(\epsilon_O)\hat{Q}_{mN}/\hat{Q}_{mO}.$$

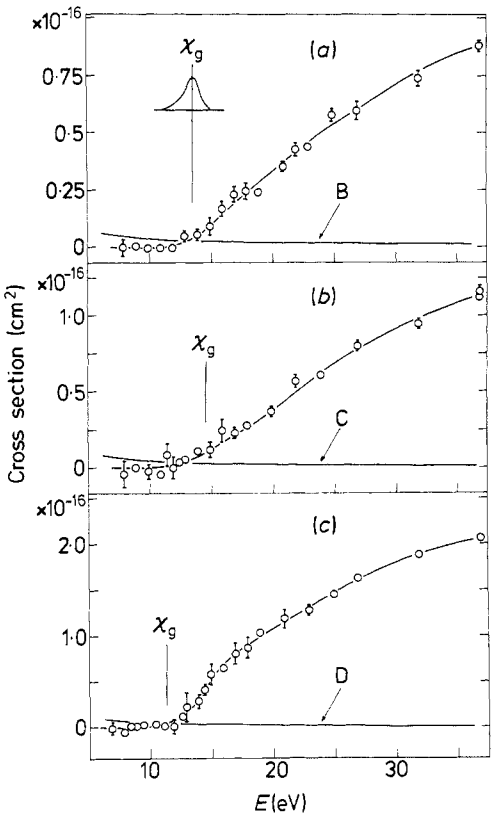

Figure 4. Ionisation at low energies of (*a*) oxygen, (*b*) nitrogen and (*c*) carbon atoms. Data for $Q(E)$ measured with 2 keV atom beams are shown by ○ and the error bars represent 90% confidence limits where these are larger than the symbol. The apparent cross sections for ionisation of long-lived excited atoms in the beams are shown by curves B, C and D and are described in the text. The approximate distribution of electron energies around their mean is shown inset in figure 4(*a*) at the ground-state threshold energy χ_g.

Here the subscripts N and O refer to the two atomic species, ϵ is the incident electron energy expressed in units of the appropriate ground-state threshold energy and $\hat{Q}_m$ is the peak value of the measured cross sections. The apparent cross section for the N atom beam determined in this manner is shown by curve C of figure 4(*b*) where $Q(E)$ is also shown. The cross sections for both $Q_m(E)$ and $Q(E)$ are listed in table 5. Although the apparent cross section is only 0·4% of the peak value of $Q_m(E)$ and furthermore its determination in the case of the N beam is somewhat subjective, it nevertheless provides a useful aid in identifying ionisation from metastable atoms. The data for $Q(E)$ shows a slight onset of ionisation from metastable atoms and, within the limits of uncertainty of the energy resolution, the predominant contribution appears to be from those in the ^{2}D state. As can be seen from the smooth curve drawn through the data in figure 4(*b*), the main contribution to ionisation occurs at the ^{4}S ground-state threshold (14·5 eV) and there is evidence of a further increase at the threshold for inner-shell ionisation from the ground state

Table 4. Electron impact ionisation of atomic oxygen.

Mean electron energy† (eV)	$Q_m(E)$ (10^{-16} cm^2)	$Q(E)$‡ (10^{-16} cm^2)	Random errors§ (10^{-16} cm^2)
7·9*	0·047	−0·001	0·036
8·9*	0·050	0·007	0·015
9·9*	0·033	−0·006	0·018
10·9*	0·034	−0·001	0·017
11·9*	0·030	−0·002	0·012
(a)			
12·9*	0·077	0·047	0·022
13·9*	0·085	0·057	0·024
14·9*	0·119	0·093	0·039
15·9*	0·194	0·170	0·032
16·9*	0·254	0·231	0·034
17·9*	0·267	0·246	0·038
18·9*	0·261	0·241	0·020
20·9*	0·371	0·353	0·022
21·9*	0·444	0·427	0·029
22·9*	0·456	0·439	0·013
24·9*	0·591	0·576	0·027
26·9*	0·610	0·596	0·041
31·9*	0·747	0·735	0·034
(b)			
36·9*	0·889	0·879	0·026
47*	1·075	1·067	0·012
47	1·145	1·137	0·037
57*	1·230	1·223	0·022
72*	1·308	1·303	0·009
97*	1·360	1·356	0·005
97	1·305	1·301	0·011
122*	1·337	1·334	0·003
147*	1·284	1·281	0·004
147	1·327	1·324	0·023
197	1·241	1·239	0·007
247*	1·095	1·093	0·006
297*	0·995	0·994	0·004
297	1·051	1·050	0·007
397*	0·864	0·863	0·004
397	0·817	0·816	0·007
497	0·785	0·784	0·004
597	0·687	0·686	0·012
797	0·571	0·571	0·006
997	0·482	0·482	0·007

(b) All measurements below (b) were made absolute by normalisation to the absolute value of $Q_m(E)$ measured at 36·9 eV using a 2 keV beam.
* Data obtained using a 2 keV atom beam. All other data were obtained using a 4 keV atom beam. All data were obtained with only the electron beam pulsed.
Other footnotes as for table 2.

(20·4 eV). Any contributions from autoionisation or from inner-shell ionisation of metastable atoms cannot be distinguished.

The carbon atom also has thresholds for ionisation from metastable states that lie below the ^{3}P ground-state threshold at 11·26 eV. Thus the low-energy data

Table 5. Electron impact ionisation of atomic nitrogen.

Mean electron energy† (eV)	$Q_m(E)$ (10^{-16} cm^2)	$Q(E)$‖ (10^{-16} cm^2)	Random errors§ (10^{-16} cm^2)
7·9*	0·023	−0·038	0·089
8·9*	0·058	0·004	0·014
9·9*	0·029	−0·020	0·051
10·9*	0·001	−0·043	0·009
11·4*	0·130	0·087	0·079
11·9*	0·048	0·007	0·072
12·4*	0·074	0·035	0·035
12·9*	0·092	0·054	0·022
13·9*	0·148	0·113	0·020
14·9*	0·155	0·122	0·050
15·9*	0·279	0·248	0·079
16·9*	0·261	0·232	0·037
17·9*	0·307	0·280	0·022
19·9*	0·396	0·372	0·033
21·9*	0·590	0·568	0·042
23·9*	0·628	0·608	0·028
26·9*	0·817	0·799	0·033
31·9*	0·960	0·945	0·033
(b)			
36·9*	1·170	1·157	0·040
37	1·130	1·117	0·023
47	1·351	1·341	0·025
67	1·520	1·513	0·023
77	1·596	1·590	0·030
87*	1.614	1·608	0·013
97	1·591	1·586	0·013
147*	1·448	1·445	0·033
147	1·448	1·445	0·004
197	1·291	1·289	0·012
297	1·099	1·097	0·012
397	0·915	0·914	0·015
497	0·817	0·816	0·015
597	0·698	0·697	0·006
797	0·587	0·587	0·007
997	0·490	0·490	0·008

‖ The apparent cross section used to determine $Q(E)$ was estimated from scaled data for the oxygen atom beam as described in the text.
Other footnotes as for table 4.

obtained using a carbon beam were treated in a manner similar to that used for the nitrogen data. The apparent cross section for this beam amounts to only 0·3% of the peak value of $Q_m(E)$ and it is shown by curve D of figure 4(*c*). $Q(E)$ is shown in figure 4(*c*) and is listed together with $Q_m(E)$ in table 6. There is no evidence of ionisation of metastable atoms, so that the onset corresponds to the ground-state threshold. At energies slightly above the ground-state threshold there is a substantial increase in ionisation presumably due to contributions arising from excitation of the ^{1}D autoionising state at 12·1 eV. However, there is an interesting reduction in the slope of the ionisation cross section at about 17·5 eV. A plausible hypothesis

Table 6. Electron impact ionisation of carbon.

Mean electron energy† (eV)	$Q_m(E)$ (10^{-16} cm^2)	$Q(E)_{\|\|}$ (10^{-16} cm^2)	Random errors§ (10^{-16} cm^2)
6·9*	0·063	−0·015	0·058
7·9*	0·012	−0·056	0·048
8·4*	0·075	0·011	0·028
8·9*	0·070	0·009	0·023
9·4*	0·090	0·032	0·045
10·4*	0·084	0·032	0·038
11·1*	0·068	0·019	0·040
11·9*	0·055	0·010	0·072
12·6*	0·159	0·116	0·031
12·9*	0·267	0·225	0·164
13·9*	0·322	0·283	0·079
14·4*	0·450	0·412	0·061
14·9*	0·617	0·581	0·119
15·9*	0·687	0·653	0·036
16·9*	0·832	0·800	0·116
17·9*	0·902	0·872	0·119
18·9*	1·066	1·037	0·039
20·9*	1·210	1·184	0·108
22·9*	1·306	1·282	0·058
24·9*	1·473	1·451	0·017
26·9*	1·650	1·630	0·039
31·9*	1·899	1·882	0·041
(b)			
36·9*	2·088	2·073	0·018
37	2·057	2·042	0·012
47*	2·227	2·215	0·034
57*	2·318	2·309	0·034
57	2·248	2·239	0·037
67*	2·323	2·315	0·022
77	2·241	2·234	0·017
87*	2·199	2·193	0·060
97	2·124	2·118	0·019
107*	2·108	2·103	0·033
137*	1·913	1·909	0·015
147	1·838	1·834	0·040
172*	1·768	1·765	0·011
197	1·611	1·608	0·038
207*	1·617	1·614	0·012
247	1·533	1·531	0·008
297	1·312	1·310	0·007
347*	1·222	1·220	0·009
397	1·118	1·117	0·017
497	0·995	0·994	0·011
597	0·875	0·874	0·028
697*	0·745	0·744	0·013
797	0·728	0·727	0·014
997	0·597	0·596	0·007

Footnotes as for table 5.

is that between 12·1 and 17·5 eV autoionisation arises predominantly from the spin-disallowed $^3P \rightarrow {}^1D$ transition whose excitation cross section, after rising to a sharp peak, is decreasing with energy at 17·5 eV. At this energy the dominant autoionising channel becomes the optically allowed $^3P \rightarrow {}^3D$ transition whose excitation cross section exhibits a gentle rise from its threshold of 13·1 eV to a peak at higher energy, in the manner normal to such allowed transitions. Ionisation contributions arising from inner-shell ionisation of ground-state C cannot be distinguished, possibly because of the large magnitude of the autoionisation contribution.

Large contributions from autoionisation are to be expected for the carbon atom because both the optically allowed and disallowed transitions from the ground to autoionising states correspond to $\Delta n = 0$ and so are likely to have large cross sections. Conversely the transitions in both O and N atoms are optically allowed but have $\Delta n = 1$ and are presumably much less probable.

Only in the low-energy data for the N atom beam is there clear evidence of metastable atoms. However, the ionisation cross sections of metastable atoms of O, N and C are only slightly larger than those for the ground-state atoms (about 5%; see Peach 1970, 1971). Thus the presence of metastable atoms in any of the beams is not likely to have caused the measured data to differ significantly from those of a beam of ground-state atoms.

3.3. Comparison with experiment and theory

The present $Q(E)$ data for O, N and C atoms are plotted together with data from other experiments and from theoretical calculations in figures 5, 6 and 7 respectively.

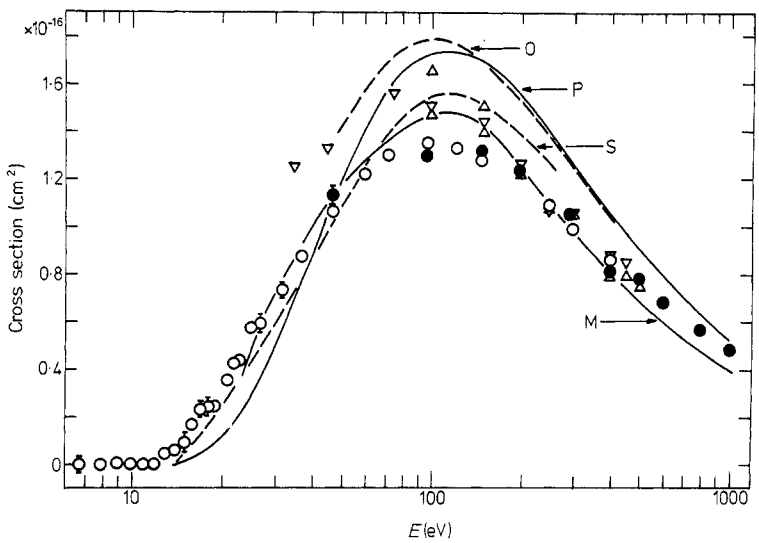

Figure 5. Electron impact ionisation cross sections for ground-state oxygen atoms. Data for $Q(E)$ measured with 2 keV atom beams are shown by ○ and for 4 keV beams by ●. The error bars represent 90% confidence limits where these are larger than the symbol and are only shown for the present fast atom beam data. The results of Fite and Brackmann (1959) are shown by ▽ and those of Rothe *et al* (1962) by △. The theoretical cross sections are: curve P, Peach (1970, 1971); O, Omidvar *et al* (1972); M, McGuire (1972); S, Seaton (1959).

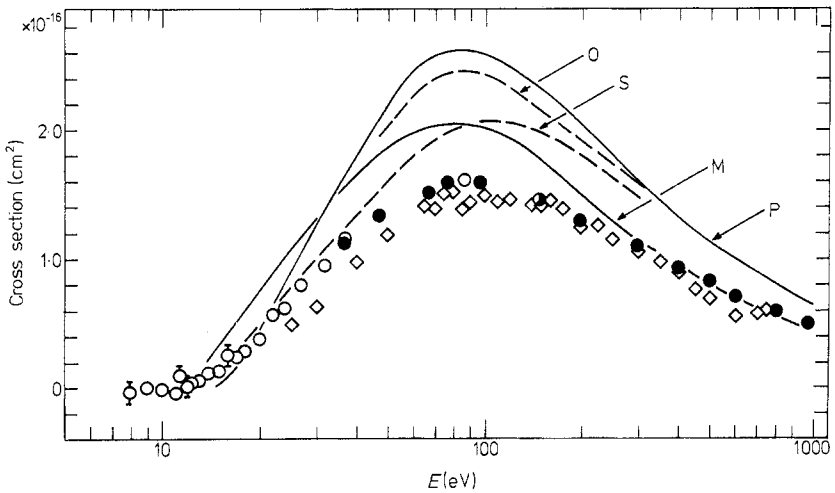

Figure 6. Electron impact ionisation cross sections for ground-state nitrogen atoms. The data of Smith *et al* (1962) are shown by ◇, other symbols are the same as for figure 5.

Data for oxygen atoms obtained in two thermal atom/crossed electron beam experiments are plotted in figure 5, namely those of Fite and Brackmann (1959) and Rothe *et al* (1962). Both experiments used partially dissociated beams of molecules and each apparatus was calibrated by normalisation to the electron impact ionisation data of Tate and Smith (1932) for O_2 molecules. The high-energy data from both experiments (150 to 500 eV) agree well with the present data but at lower energies both of the thermal-beam experiments yield larger cross sections. If these relative

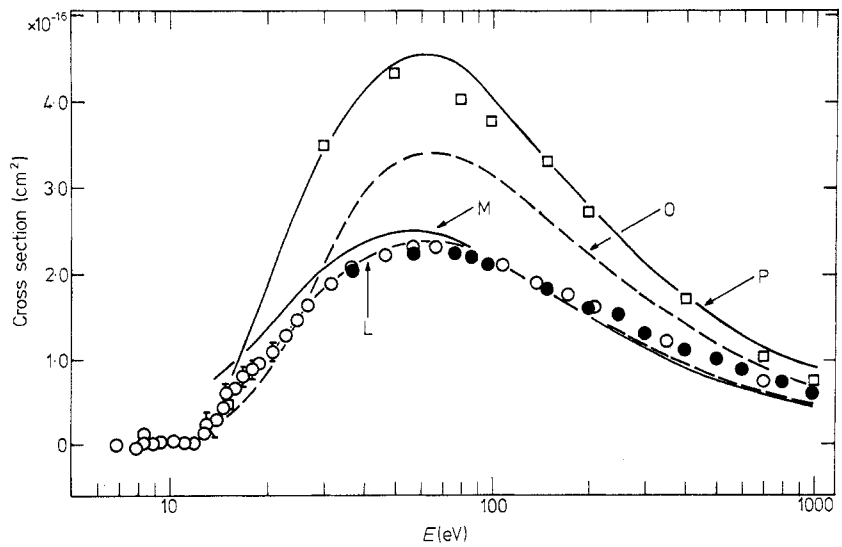

Figure 7. Electron impact ionisation cross sections for ground-state carbon atoms. The data of Wang and Crawford (1971) are shown by □ and the semi-empirical calculation of Lotz (1968) which includes inner-shell ionisation, by curve L. Other symbols are the same as for figure 5.

experiments had been normalised to the more recent (and probably more accurate) data for O_2 molecules measured by Rapp and Englander-Golden, then they would be in much better agreement with the present fast atom beam data.

The data of Smith *et al* (1962) for N atoms were obtained using the same basic apparatus and normalisation procedure as were used by Rothe *et al* for O atoms. In the energy regime 150 to 400 eV there is good agreement with the present data but at low energies the thermal-beam data should also overestimate the cross section because it was normalised to the N_2 molecular data of Tate and Smith rather than those of Rapp and Englander-Golden. However, the reverse appears to be the case and two further aspects should be noted. Firstly, at energies above 600 eV the cross section for N atoms measured by Smith *et al* increases with increasing energy and this is most unlikely to be a feature of the ionisation process. Secondly, two different electron guns were used and the low-energy data that lie below the present results were obtained using a gun in which the electron beam was magnetically collimated. More detailed analysis of these early experiments is not profitable; suffice it to state that the considerable uncertainties in their normalisation, in the reproducibility of data and in their collection efficiency of the product ions are more than adequate to account for the deviations from the present data; indeed the agreement is impressively good. There are two further relevant experiments, that of Boksenberg (1961) for thermal-beam data on O atoms and of Peterson (1964) for fast-beam data on N atoms. Neither is plotted because they are clearly incorrect and both exceed the present measurements by about 100%. These inaccuracies notwithstanding, the present experiments owe much to Peterson's pioneering work.

In the case of C atoms the experimental data of Wang and Crawford (1971) are plotted for comparison with the present data. There is substantial disagreement but Wang and Crawford claim an accuracy of only $\pm 30\%$. Further consideration is not practicable because details of the work are not available.

Peach used the Born–Ochkur approximation to calculate cross sections for outer-shell ionisation from the ground state (Peach 1971) and also for the inner shell with autoionisation from the ground state (Peach 1970). The sums of these cross sections are plotted here for the O, N and C atoms. Agreement is best for O atoms where the theoretical cross section is larger by about 30% at the peak and remains some 6% high at 1000 eV. However, the calculated cross sections are progressively larger for N and C atoms. One possible reason is that the theory overestimates contributions from the inner shell and autoionisation. The present experimental data show only slight evidence of inner-shell ionisation and no discernible evidence of autoionisation for O and N atoms. Only for C atoms can autoionisation be clearly seen and here it is so large that it masks any contribution from inner-shell ionisation.

The Born approximation used for O, N and C atoms by Omidvar *et al* (1972) overestimates the peak and high-energy cross sections by about the same proportion for each atom. However, these authors state that their approach is likely to overestimate the high-energy cross sections for atoms in the present range of atomic numbers. The calculations of McGuire (1971) are based upon a generalised oscillator strength formulation of the Born approximation. These are in somewhat better agreement for each atom at the peak and at high energies, but the calculations have little meaning close to threshold because non-physical values of the ionisation thresholds were used. A similar approach was taken for O atoms by Kazaks *et al* (1972) but their data are not plotted here because they are barely distinguishable from those of Peach and Omidvar. The empirically scaled Bethe approximation used by Seaton

(1959) is in quite good agreement with the low-energy data for O atoms but is less successful in the case of N atoms.

The semi-empirical calculations of Lotz (1968) are not plotted for O or N atoms because his empirical parameters were fitted to the early thermal atom-beam data and so must be adjusted to agree with the present data. Nevertheless the calculation of Lotz for C atoms is in good agreement with the present data.

Acknowledgments

The authors wish to thank Dr R S Pease, the Director of Culham Laboratory, for supporting this study. We are also indebted to Messrs P R White, G H Hirst and D A Hobbis for their skilled assistance. One of us (EB) is grateful for financial support provided by the United Kingdom Atomic Energy Authority throughout the course of this work.

References

Barnett C F, Ray J A, Ricci E, Wilker M I, McDaniel E W, Thomas E W and Gilbody H B 1977 *Atomic Data for Controlled Fusion Research* Oak Ridge National Laboratory Report ORNL-5207

Boksenberg A 1961 *PhD Thesis* University of London

Crawford C K and Wang K I 1967 *J. Chem. Phys.* **47** 4667–9

Dance D F, Harrison M F A and Rundel R D 1967 *Proc. R. Soc.* A **299** 525–37

Dance D F, Harrison M F A and Smith A C H 1966 *Proc. R. Soc.* A **290** 74–93

Dixon A J, von Engel A and Harrison M F A 1975 *Proc. R. Soc.* A **343** 333–49

Dixon A J, Harrison M F A and Smith A C H 1976 *J. Phys. B: Atom. Molec. Phys.* **9** 2617–31

Fite W L and Brackmann R T 1959 *Phys. Rev.* **113** 815–6

Harrison M F A 1968 *Methods of Experimental Physics* vol 7A, ed B Bederson and W L Fite (New York: Academic Press) pp 95–115

——1977 *Atomic and Molecular Data for Fusion* International Atomic Energy Agency, Vienna, Technical Report IAEA-199, pp 81–113

Harrison M F A, Dolder K T and Thonemann P C 1963 *Proc. Phys. Soc.* **82** 368–71

Kazaks P A, Ganas P S and Green A E S 1972 *Phys. Rev.* A **6** 2169–80

Kieffer L J and Dunn G H 1966 *Rev. Mod. Phys.* **38** 1–35

Lotz W 1968 *Z. Phys.* **216** 241–7

McGuire E J 1971 *Phys. Rev.* A **3** 267–79

Omidvar K, Kyle H L and Sullivan E C 1972 *Phys. Rev.* A **5** 1174–87

Peach G 1970 *J. Phys. B: Atom. Molec. Phys.* **3** 328–49

——1971 *J. Phys. B: Atom. Molec. Phys.* **4** 1670–7

Peterson J R 1964 *Atomic Collision Processes* ed M R C McDowell (Amsterdam: North-Holland) pp 465–73

Rapp D and Englander-Golden P 1965 *J. Chem. Phys.* **43** 1464–79

Rothe E W, Marino L L, Neynaber R H and Trujillo S M 1962 *Phys. Rev.* **125** 582–3

Seaton M J 1959 *Phys. Rev.* **113** 814

Smith A C H, Caplinger E, Neynaber R H, Rothe E W and Trujillo S M 1962 *Phys. Rev.* **127** 1647–9

Stanton H E and Monahan J E 1960 *Phys. Rev.* **119** 711–5

Tate J T and Smith P T 1932 *Phys. Rev.* **39** 270–7

Wang K I and Crawford C K 1971 *Electron Impact Ionization Cross Sections* Particle Optics Lab, MIT, Technical Report No 6, AFML-TR-70-289